

# Eriodictyol Inhibits RANKL-Induced Osteoclast Formation and Function Via Inhibition of NFATc1 Activity

FANGMING SONG,<sup>1,2,3</sup> LIN ZHOU,<sup>2</sup> JINMIN ZHAO,<sup>1,4</sup> QIAN LIU,<sup>1,4</sup> MINGLI YANG,<sup>2</sup> RENXIANG TAN,<sup>5</sup> JUN XU,<sup>6</sup> GE ZHANG,<sup>7</sup> JULIAN M.W. QUINN,<sup>8</sup> JENNIFER TICKNER,<sup>2</sup> YUANJIAO HUANG,<sup>1,9\*</sup> AND JIAKE XU<sup>1,2,\*\*</sup>

<sup>1</sup>Department of Biochemistry and Molecular Biology, Key Laboratory of Biological Molecular Medicine Research of Guangxi Higher Education, Guangxi Key Laboratory of Regenerative Medicine, Guangxi Medical University, Nanning, Guangxi, China

<sup>2</sup>School of Pathology and Laboratory Medicine, The University of Western Australia, Perth, Western Australia, Australia

<sup>3</sup>Pharmaceutical College, Guangxi Medical University, Nanning, Guangxi, China

<sup>4</sup>Department of Orthopaedic Surgery, The First Affiliated Hospital of Guangxi Medical University, Nanning, Guangxi, China

<sup>5</sup>Institute of Functional Biomolecules, Medical School, Nanjing University, Nanjing, Jiangsu, China

<sup>6</sup>Research Center for Drug Discovery (RCDD), School of Pharmaceutical Sciences, Sun Yat-Sen University, Guangzhou, Guangdong, China

<sup>7</sup>Institute for Advancing Translational Medicine in Bone and Joint Diseases, School of Chinese Medicine, Hong Kong Baptist University, Hong Kong, China

<sup>8</sup>The Garvan Institute of Medical Research, Darlinghurst, New South Wales, Australia

<sup>9</sup>Medical Scientific Research Center, Guangxi Medical University, Nanning, Guangxi, China

Receptor activator of nuclear factor kappa-B ligand (RANKL) induces differentiation and function of osteoclasts through triggering multiple signaling cascades, including NF- $\kappa$ B, MAPK, and Ca<sup>2+</sup>-dependent signals, which induce and activate critical transcription factor NFATc1. Targeting these signaling cascades may serve as an effective therapy against osteoclast-related diseases. Here, by screening a panel of natural plant extracts with known anti-inflammatory, anti-tumor, or anti-oxidant properties for possible anti-osteoclastogenic activities we identified Eriodictyol. This flavanone potently suppressed RANKL-induced osteoclastogenesis and bone resorption in a dose-dependent manner without detectable cytotoxicity, suppressing RANKL-induced NF- $\kappa$ B, MAPK, and Ca<sup>2+</sup> signaling pathways. Eriodictyol also strongly inhibited RANKL-induction of c-Fos levels (a critical component of AP-1 transcription factor required by osteoclasts) and subsequent activation of NFATc1, concomitant with reduced expression of osteoclast specific genes including cathepsin K (Ctsk), V-ATPase-d2 subunit, and tartrate resistant acid phosphatase (TRAcP/Acp5). Taken together, these data provide evidence that Eriodictyol could be useful for the prevention and treatment of osteolytic disorders associated with abnormally increased osteoclast formation and function.

J. Cell. Physiol. 231: 1983–1993, 2016. © 2016 Wiley Periodicals, Inc.

Bone is a dynamic and living organ, which continuously undergoes the process of repair and renewal throughout life (Teitelbaum, 2000). This process involves osteoblast activity (bone formation) and osteoclast activity (bone resorption).

However, bone disorders, such as osteoporosis and Paget's disease of bone, are characterized by bone loss owing to the excessive formation and production of osteoclasts (Manolagas and Jilka, 1995; Kular et al., 2012).

Fangming Song and Lin Zhou contributed equally to this work.

Fangming Song and Jiake Xu made mutual collaborative visits in 2015.

Contract grant sponsor: National Health and Medical Research Council of Australia, Natural Science Foundation of Guangxi Province;

Contract grant number: No. 2015GXNSFDA139019.

Contract grant sponsor: Innovation Project of Guangxi Graduate Education.

Contract grant sponsor: Co-innovation Centre for Bio-Medicine, Guangxi Key Laboratory of Regenerative Medicine, Guangxi Medical University.

\*Correspondence to: Yuanjiao Huang, Department of Biochemistry and Molecular Biology, Key Laboratory of Biological Molecular

Medicine Research of Guangxi Higher Education, Medical Scientific Research Center, Guangxi Medical University, Guangxi, China.

E-mail: hyjxm@126.com

\*\*Correspondence to: Jiake Xu, School of Pathology and Laboratory Medicine, The University of Western Australia, Perth, Western Australia, Australia. E-mail: jiake.xu@uwa.edu.au

Manuscript Received: 26 November 2015

Manuscript Accepted: 6 January 2016

Accepted manuscript online in Wiley Online Library (wileyonlinelibrary.com): 11 January 2016.

DOI: 10.1002/jcp.25304

Osteoclasts are multinuclear cells that are derived from the differentiation of monocyte/macrophage lineage hematopoietic cells. The process of macrophage differentiation into osteoclasts depends on two essential cytokines: macrophage colony-stimulating factor (M-CSF) and receptor activator of nuclear factor kappa B (NF- $\kappa$ B) ligand (RANKL) (Boyle et al., 2003). RANKL is a key cytokine for osteoclast differentiation, function, and survival, and exerts its biological effects through interacting with its receptor, Receptor activator of NF- $\kappa$ B (RANK). The binding of RANKL to RANK results in activation of MAPK, NF- $\kappa$ B, and Ca<sup>2+</sup> signal transduction pathways followed by stimulation of several transcription factors, such as c-Fos and NFATc1, which are indispensable for osteoclastogenesis (Baud'huin et al., 2007). Osteoclast-specific gene expression is initiated by NFATc1 in response to RANKL stimulation (Negishi-Koga and Takayanagi, 2009). M-CSF is a key factor responsible for inducing survival and proliferation of osteoclast precursors. M-CSF can also modulate the levels of RANK in bone marrow macrophage cells (BMMs) sensitizing them to RANKL stimulation (Takayanagi, 2007). Thus, impairment of RANKL-induced molecular and signaling pathways can be useful for the treatment of osteoclast-related disease.

Eriodictyol, a flavonoid extracted from plants such as *Citrus limon*, has a wide range of biomedical and pharmacological effects, which include antioxidant (Lee et al., 2015) and anti-inflammatory activities (Lee, 2011; Lee et al., 2013). However, the cellular and molecular actions of Eriodictyol on RANKL-induced osteoclast formation and function are not clear. In order to assess the impact of Eriodictyol on RANKL-mediated osteoclastogenesis, we investigated the effects and mechanism of action of Eriodictyol in regulating formation and function of osteoclasts. Our results demonstrate that Eriodictyol is capable of inhibiting RANKL-induced osteoclastogenesis and bone resorption through suppression of NFATc1 activation via NF- $\kappa$ B, MAPK, and Ca<sup>2+</sup> signaling pathways. Collectively, these data suggest that Eriodictyol is a novel and potential candidate for treatment of osteolytic bone diseases.

## Materials and Methods

### Materials

Alpha modified Minimal Essential Medium ( $\alpha$ -MEM) and fetal bovine serum (FBS) was purchased from Thermo Fisher Scientific (Scoresby, Australia). Eriodictyol with a purity >95% was purchased from the National Institute for Control of Pharmaceutical and Biological Products (Beijing, China) and prepared at a concentration of 100  $\mu$ M in Dimethyl sulfoxide (DMSO). DMSO alone was used as vehicle in these assays and shows no effect. Antibodies specific for NFATc1, I $\kappa$ B $\alpha$ , ERK, JNK, p38, phosphorylated (p) ERK, p-p38, p-JNK, and  $\beta$ -actin were obtained from Santa Cruz Biotechnology (San Jose, CA). Vacuolar-type H<sup>+</sup>-ATPase V0 subunit d2 (V-ATPase d2) was generated as previously described (Feng et al., 2009). The MTS and luciferase assay system were obtained from Promega (Sydney, Australia). Recombinant macrophage colony stimulating factor (M-CSF) was obtained from R&D Systems (Minneapolis, MN). Leucocyte acid phosphatase staining kits were obtained from Sigma-Aldrich (Sydney, Australia). Recombinant GST-rRANKL protein was expressed and purified as previously described (Xu et al., 2000).

### Cell culture

RAW264.7 cells (mouse macrophage cells) were obtained from the American Type Culture Collection (Manassas, VA) and cultured in  $\alpha$ -MEM supplemented with 10% FBS, 2 mM L-glutamine, 100 units/mL penicillin, and 100 g/mL streptomycin (complete

medium). Bone marrow macrophage cells (BMMs) were isolated from 6-week-old C57BL/6J mice by flushing the marrow from the femur and tibia, and then culture in complete medium in the presence of M-CSF (50 ng/mL).

### Drug screening assay and osteoclastogenesis assay

Drug screening assays were conducted using BMMs isolated as described above to evaluate RANKL-induced osteoclastogenesis. BMMs were plated into 96-well culture plates at a density of  $6 \times 10^3$  cells/well, and treated with complete medium containing M-CSF and GST-rRANKL (50 ng/mL) in the presence or absence of natural compounds (screening assay–10  $\mu$ M) or varying concentrations of Eriodictyol. The cell culture medium was changed every 2 days. After 5 days, cells were fixed with 4% paraformaldehyde for 10 min, washed three times with PBS, and then stained for tartrate resistant acid phosphatase (TRAcP) enzymatic activity using a leucocyte acid phosphatase staining kit (Sigma-Aldrich, Sydney, Australia), following the manufacturer's procedures. TRAcP-positive multinucleated cells (>3 nuclei) were counted as osteoclasts.

### Cytotoxicity assays

BMMs were seeded into a 96-well plate at  $6 \times 10^3$  cell/well and left overnight to adhere. The following day, the cells were incubated with varying concentrations of Eriodictyol for 48 h. At the end of the experiment, MTS solution (20  $\mu$ L/well) was added and incubated with cells for 2 h. The absorbance at 490 nm was read with a microplate reader (Thermo LabSystem Multiscan Spectrum, Thermo labSystem, Chantilly, VA).

### Hydroxyapatite resorption assay

To measure osteoclast activity, osteoclasts were first generated from BMMs ( $1 \times 10^5$  cells per well) cultured onto 6-well collagen-coated plates and stimulated with 50 ng/mL GST-rRANKL and M-CSF until mature osteoclasts were generated. Cells were gently detached from the plate using cell dissociation solution (Sigma-Aldrich, Sydney, Australia) and mature osteoclasts were seeded into individual wells in hydroxyapatite-coated 96-well plates (Corning, Inc., Corning, NY). Starting osteoclast number was the same in each well. Mature osteoclasts were incubated in medium containing GST-rRANKL and M-CSF with or without Eriodictyol at the indicated concentration. After 48 h, half of the wells were histochemically stained for TRAcP activity as above to assess the number of multinucleated cells per well. The remaining wells were bleached for 10 min to remove the cells and allow measurement of the resorbed areas, which were photographed under standard light microscopy. ImageJ software (NIH, Bethesda, MD) to quantify the percentage area of hydroxyapatite surface resorbed by the osteoclasts.

### Luciferase reporter assays

To investigate NF- $\kappa$ B and NFATc1 transcriptional activation, RAW264.7 cells were stably transfected with either an NF- $\kappa$ B-responsive luciferase construct (Wang et al., 2003) or an NFATc1-responsive luciferase reporter construct (van der Kraan et al., 2013). Transfected cells were cultured in 48-well plates at a density of  $1.5 \times 10^5$  cells/well (NF- $\kappa$ B luciferase report gene assay) or  $5 \times 10^4$  cells/well (NFATc1 luciferase report gene assay), respectively, and pretreated with various concentrations of Eriodictyol for 1 h. Following pre-treatment cells were subsequently stimulated with GST-rRANKL (50 ng/mL) for 6 h (NF- $\kappa$ B luciferase report gene assay) or 24 h (NFAT luciferase reporter gene assay) and luciferase activity was detected using the

TABLE 1. The effect of natural compounds on RANKL-induced osteoclastogenesis

Compounds name	Origins	Inhibitory effect on RANKL-induced Osteoclast number (IC50)
Eriodictyol	Natural	IC50 ≈ 5 μM
Sinapine thiocyanate	Natural	IC50 > 10 μM or no effect
Jervine	Natural	IC50 > 10 μM or no effect
Veratramine	Natural	IC50 > 10 μM or no effect
Olaquinox	Natural	IC50 > 10 μM or no effect
Pedunculoside	Natural	IC50 > 10 μM or no effect
Barbaloin	Natural	IC50 > 10 μM or no effect
Orcinoglucosid	Natural	IC50 > 10 μM or no effect
Betulin	Natural	IC50 > 10 μM or no effect
Germacrone	Natural	IC50 > 10 μM or no effect
Paeoniflorin	Natural	IC50 > 10 μM or no effect
Albiflorin	Natural	IC50 > 10 μM or no effect
Alpinetin	Natural	IC50 > 10 μM or no effect
Calycosin	Natural	IC50 > 10 μM or no effect
Tectorigenin	Natural	IC50 > 10 μM or no effect
Matrine	Natural	IC50 > 10 μM or no effect
Arbutin	Natural	IC50 > 10 μM or no effect
Hydroxyocholic acid	Natural	IC50 > 10 μM or no effect
Ethyl ferulate	Natural	IC50 > 10 μM or no effect
L-Rhamnose	Natural	IC50 > 10 μM or no effect
Ligustrazine hydrochloride	Natural	IC50 > 10 μM or no effect

luciferase reporter assay system according to the manufacturer's protocol (Promega, Sydney, Australia).

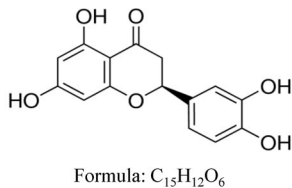
### Reverse transcription (RT)-PCR analysis of gene expression

Total RNA was isolated from cells using Trizol reagent according to the manufacturer's protocol (ThermoFisher Scientific, Scoresby Australia). The cDNA was synthesized using Moloney murine leukemia virus reverse transcriptase with 1 μg of RNA template and oligo-dT primers. Polymerase chain reaction amplification of specific sequences was performed using the following cycle: 94°C for 5 min, followed by 30 cycles of 94°C for 40 sec, 60°C for 40 sec, and 72°C for 40 sec, and a final extension step of 5 min at 72°C. Reaction products (8 μL) were separated using agarose gel electrophoresis and visualized on an Image-quant LAS 4000 (GE Healthcare, Silverwater, Australia) and analyzed by ImageJ software.

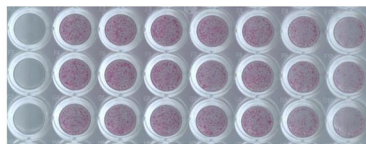
The following specific primers (based on the mouse sequences) were used:

cathepsin K (Ctsk) (Forward: 5'-GGGAGAAAAACCT-GAAGC-3'; Reverse: 5'-ATTCTGGGACTCAGAGC-3'), TRAcP (Acp5) (Forward: 5'-TGTGGCCATCTTTATGCT-3'; Reverse: 5'-GTCATTTCTTTGGGGCTT-3'),

A

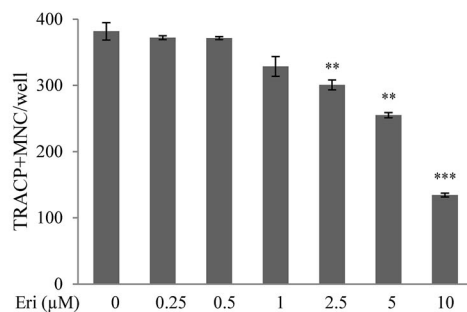


C

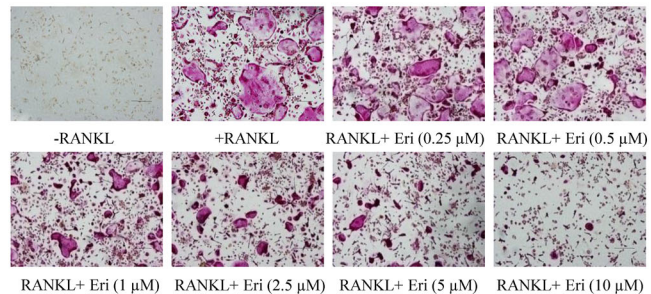


RANKL - + + + + + + +  
Eri - 0 0.25 0.5 1 2.5 5 10 μM

D



B



E

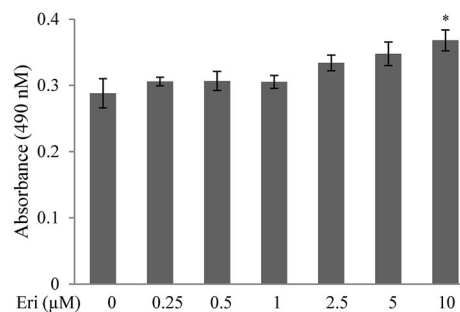


**Fig. 1. Eriodictyol suppresses RANKL-induced osteoclastogenesis.** **A:** Structure of Eriodictyol. **B:** Representative images of RANKL-induced osteoclastogenesis in the presence of indicated concentrations of Eriodictyol (Mag = 20×; scale bar, 100 μm). **C:** Low power image of TRAcP staining showing the dose dependent effect of Eriodictyol treatment. **D:** Quantification of the effect of Eriodictyol treatment on the number of TRAcP-positive multinucleated cells (nuclei > 3) (n = 3). **E:** Survival of BMMs in the presence of Eriodictyol as assessed by MTS cell viability assay (n = 3). “-” means RANKL untreated; “+” means RANKL treated. \*P < 0.05, \*\*P < 0.01, \*\*\*P < 0.001 relative to RANKL-stimulated controls.

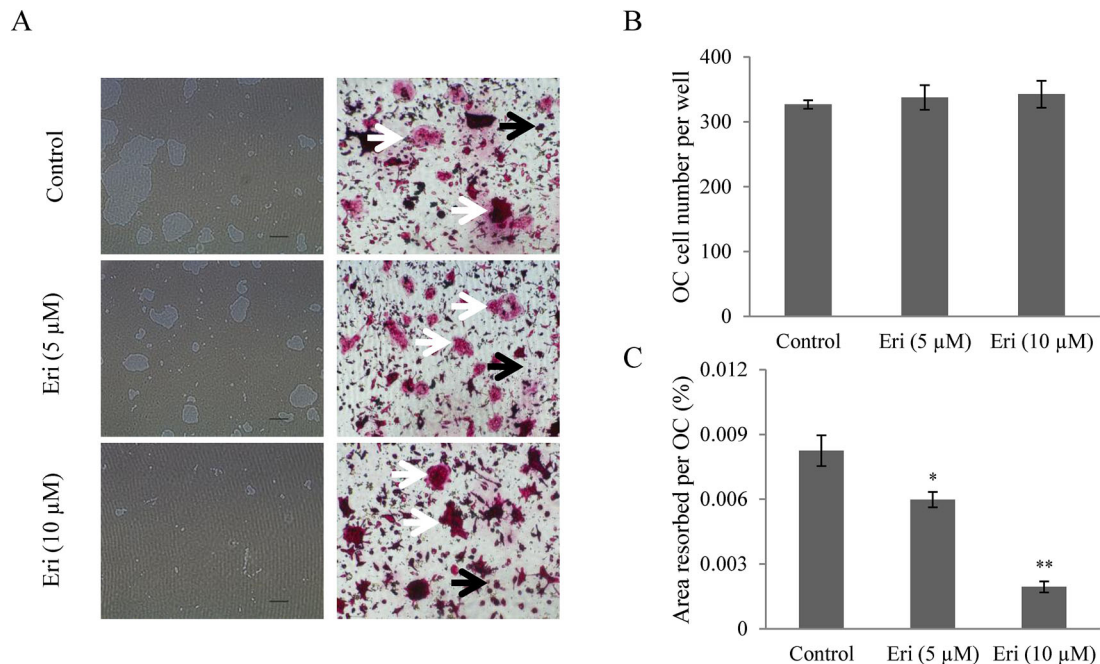


**Fig. 2.** Eriodictyol inhibits RANKL-induced hydroxyapatite resorption. **A:** Representative images of hydroxyapatite resorption (left) with corresponding TRAcP stained osteoclasts (right). White arrow indicated TRAcP-positive multinucleated cells, black arrow indicated mononuclear cells (Mag = 4×; scale bar, 500 μm). **B:** Quantification of the number of TRAcP positive cells (nuclei > 3) (n = 3). **C:** The percentage area of hydroxyapatite resorption per osteoclast (n = 3). \**P* < 0.05, \*\**P* < 0.01, \*\*\**P* < 0.001 relative to RANKL-stimulated controls.

V-ATPase-d2 (Forward: 5'-GTG AGA CCT TGG AAG ACC TGA A-3'; Reverse: 5'-GAG AAA TGT GCT CAGGGGCT-3'),  
 GAPDH (Forward: 5'-ACCACAGTCCATGCCATCAC-3'; Reverse: 5'-TCCACCACCCTGTTGCTGTA-3').

#### Western blotting

BMM cells were cultured in 6 well plates and stimulated with 100 ng/mL GST-rRANKL for the stated times. Cells were lysed in radioimmunoprecipitation (RIPA) lysis buffer, and proteins were resolved by SDS-polyacrylamide gel electrophoresis and transferred to polyvinylidene fluoride (PVDF) membranes (GE Healthcare, Silverwater, Australia). The membranes were blocked in 5% skim milk for 1 h, and then probed with various specific primary antibodies with gentle shaking overnight. Membranes were washed and subsequently incubated with horseradish peroxidase (HRP)-conjugated secondary antibodies. Antibody reactivity was then detected with enhanced chemiluminescence (ECL) reagent (Amersham Pharmacia Biotech, Piscataway, NJ), visualized on an Image-quant LAS 4000 (GE Healthcare, Silverwater, Australia) and analyzed by ImageJ software.

#### Measurement of intracellular Ca<sup>2+</sup> oscillation

Ca<sup>2+</sup> oscillations were investigated using the calcium binding dye Fluo4-AM according to the manufacturer's method (Molecular probes, Thermo Fisher Scientific, Scoresby, Australia). Briefly, BMMs were seeded into a 48-well plate at a concentration of  $1 \times 10^4$  cells/well. The following day, the medium was replaced with complete medium containing 10 μM Eriodictyol supplemented with GST-rRANKL and M-CSF for 24 h. Cells were then washed in Assay buffer (HANKS balanced salt solution supplemented with 1mM probenecid and 1% FBS) and then incubated with 4 μM Fluo4 staining solution (Fluo4-AM dissolved

in 20% pluronic-F127 (w/v) in DMSO diluted in Assay buffer, for 45 min at 37°C. Cells were washed once in Assay buffer and incubated at room temperature for 20 min followed by a further two washes in Assay buffer and visualization of fluorescence using an inverted fluorescent microscope (Nikon, Tokyo, Japan) at an excitation wavelength of 488 nm. Images were captured every 2 sec for 3 min and calcium flux analyzed using Nikon Basic Research Software. Cells that showed more than one calcium peak within the observed time frame were considered to be oscillating, with the oscillation intensity calculated as the difference between the maximum and minimum of fluorescence intensities within the oscillating cell area.

#### Statistical analysis

All experimental data are presented as the mean ± SEM and statistical significance determined by Student's *t*-test. All the experiments were repeated at least three times with results presented as the average of triplicate experiments or the data from a representative experiment that was repeated at least three times. A *P*-value < 0.05 was considered statistically significant.

## Results

### Eriodictyol inhibits osteoclastogenesis

To identify compounds that have the potential to inhibit osteoclastogenesis our preliminary screen assessed 20 natural compounds at a standardized concentration of 10 μM for their ability to inhibit RANKL-stimulated osteoclast formation from mouse BMM (Table I and Supplementary Fig. S1). From this screen we identified that Eriodictyol (Fig. 1A) exerted a strong inhibitory effect on RANKL-induced osteoclast formation. We further investigated the dose dependency of the effect of

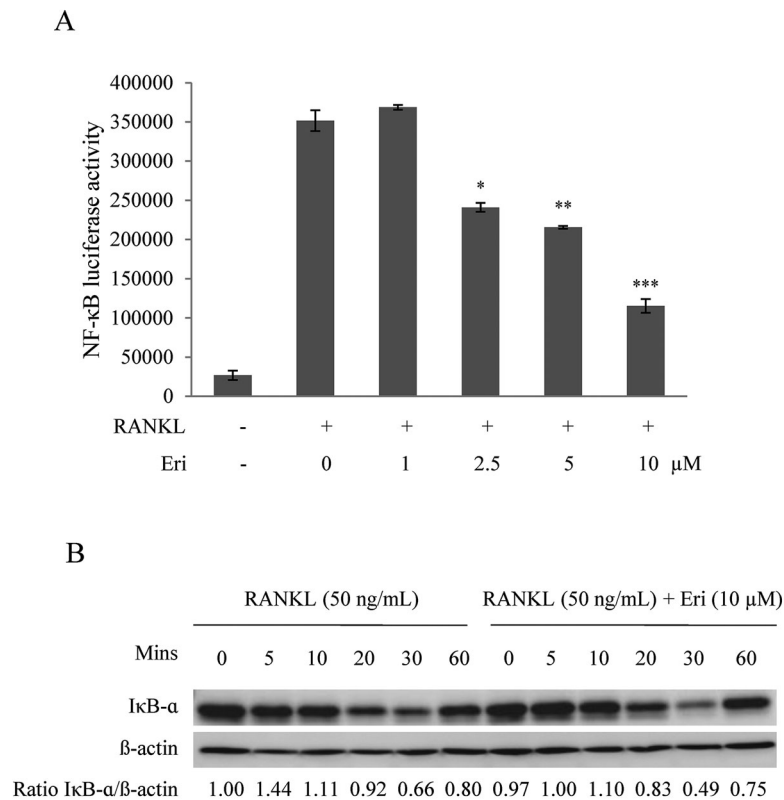


**Fig. 3.** Eriodictyol attenuates RANKL induced NF-κB activity, but has little effect on IκB-α. **A:** Luciferase activity in RANKL stimulated RAW264.7 cells transfected with an NF-κB luciferase construct. Transfected cells were pre-treated with indicated concentrations of Eriodictyol and subsequently stimulated with GST-rRANKL (50 ng/mL) ( $n = 3$ ). “-” means RANKL untreated; “+” means RANKL treated. \* $P < 0.05$ , \*\* $P < 0.01$ , \*\*\* $P < 0.001$  relative to RANKL-stimulated controls. **B:** Protein lysates from BMMs pre-treated with Eriodictyol (10 μM), followed by stimulation with GST-rRANKL (50 ng/mL) for indicated times. Western-blot was probed for IκB-α and β-actin, the amount of IκB-α was normalized to β-actin and expressed as a ratio.

Eriodictyol on osteoclast formation using BMMs cultures stimulated with RANKL and M-CSF. Increasing doses of Eriodictyol exhibited a dose-dependent inhibition on the number of TRAcP positive osteoclasts formed (Fig. 1B–D). Both the size and number of osteoclasts were significantly suppressed as the concentration of Eriodictyol increased from 2.5 to 10 μM. The inhibitory concentration (IC<sub>50</sub>) of Eriodictyol for osteoclastogenesis was approximately 5 μM (Fig. 1D). We next performed a cell viability assay to determine whether the inhibitory effect of Eriodictyol on osteoclast formation was due to cytotoxic effects. Our results showed that Eriodictyol concentrations ranging from 0.25 to 10 μM were not cytotoxic to BMMs (Fig. 1E). Collectively, these results indicate that Eriodictyol inhibits RANKL-induced osteoclastogenesis in a dose-dependent manner without causing cell cytotoxicity.

### Eriodictyol inhibits osteoclastic resorption

To investigate the effect of Eriodictyol on resorption by mature osteoclasts, a hydroxyapatite resorption assay was used. We observed a large amount of hydroxyapatite resorption in the presence of RANKL alone; however, treatment with Eriodictyol caused a visible reduction in resorption area (Fig. 2A). Consistent with the lack of cytotoxicity observed in

BMM, mature osteoclast number was not affected by treatment with Eriodictyol (Fig. 2B). However, resorption area per osteoclast was significantly reduced at 5 or 10 μM Eriodictyol (Fig. 2C), with almost complete inhibition of hydroxyapatite resorption in cultures treated with 10 μM Eriodictyol. Taken together, these data show that Eriodictyol suppresses osteoclastic resorption without affecting the survival of mature osteoclasts.

### Eriodictyol suppresses RANKL-induced NF-κB and MAPK pathways

To further elucidate the molecular mechanism by which treatment with Eriodictyol results in suppression of osteoclastogenesis, we investigated the effect of Eriodictyol on the RANKL-induced signaling pathways, NF-κB, MAPK. Activation of NF-κB, as assessed by luciferase assay, was greatly reduced, with a significant reduction in NF-κB activity at concentrations greater than 2.5 μM (Fig. 3A). To determine how Eriodictyol was impacting NF-κB activity we examined the protein levels of inhibitor of NF-κB (IκB)-α using western-blot. BMM were pre-treated with 10 μM Eriodictyol and then stimulated with RANKL and RANKL induced IκB-α degradation was analysed. As shown in Figure 3B, pretreatment with Eriodictyol failed to inhibit the degradation of IκB-α.

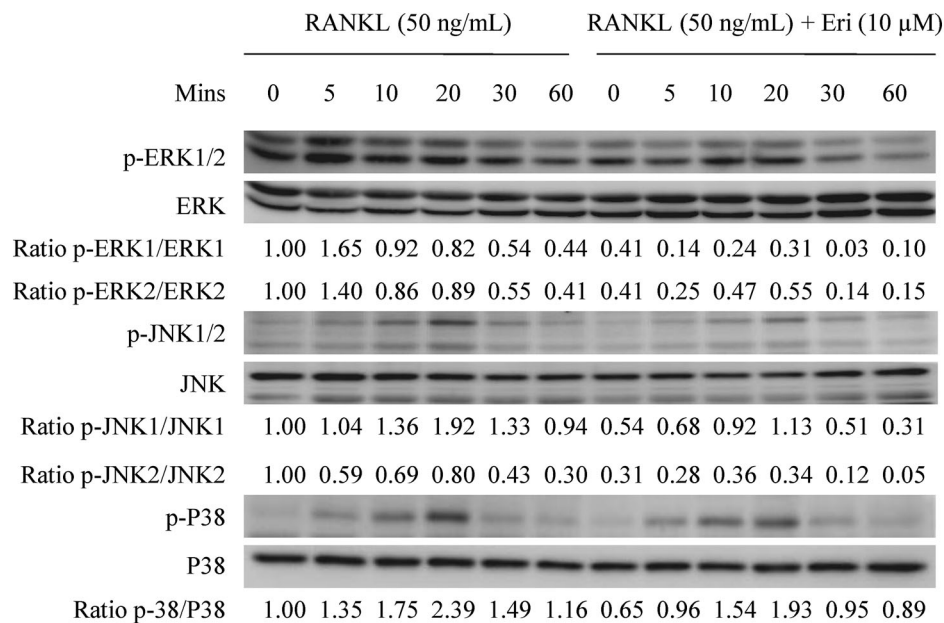


**Fig. 4.** Eriodictyol suppresses RANKL-induced phosphorylation of ERK, JNK, and P38. **A:** Protein lysates from BMMs pre-treated with Eriodictyol (10  $\mu$ M), followed by stimulation with GST-rRANKL (50 ng/mL) for indicated times. Western-blot was probed with p-ERK, ERK, p-JNK, JNK, p-P38, and P38 specific antibodies and the ratio of phosphorylated proteins relative to unphosphorylated proteins was determined.

Interestingly, we found that the phosphorylation of ERK1/2, JNK1/2, and p38 were strongly inhibited by pre-treatment with Eriodictyol, compared to untreated RANKL-induced only cells (Fig. 4A). Taken together, these findings indicate that Eriodictyol exerts an inhibitory effect on RANKL-induced activation of NF- $\kappa$ B and MAPK signaling pathways.

#### Eriodictyol inhibits RANKL-induced $Ca^{2+}$ oscillations

RANKL stimulation results in the activation of  $Ca^{2+}$  signal transduction pathways, which initiate  $Ca^{2+}$  oscillations that result in stabilization and nuclear translocation of NFATc1 transcription factor. To determine the effect of Eriodictyol on RANKL-induced  $Ca^{2+}$  signaling, intracellular  $Ca^{2+}$  oscillations were observed in RANKL stimulated BMMs. As expected, treatment with RANKL induced  $Ca^{2+}$  oscillations whereas no  $Ca^{2+}$  flux was observed in the RANKL-untreated group (Fig. 5A, B). Treatment with Eriodictyol significantly attenuated the observed RANKL induced  $Ca^{2+}$  oscillations (Fig. 5C, D). These results suggest that Eriodictyol abrogates the  $Ca^{2+}$  signaling pathway mediated by RANKL.

#### Eriodictyol represses NFATc1 and c-fos activation, and associated downstream protein expression

As  $Ca^{2+}$  oscillations are critical for activation of NFATc1, we utilized an NFATc1 luciferase reporter gene construct in RAW264.7 cells to investigate the effect of Eriodictyol on RANKL-induced NFATc1 activity. Pre-treatment with Eriodictyol resulted in a dose-dependent impairment of NFATc1 activation (Fig. 6A). Consistent with the inhibition of NFATc1 activation observed in the RAW264.7 cells, the increase in protein levels of NFATc1 observed in RANKL-stimulated BMM was notably blocked by Eriodictyol treatment on days 3 and 5 of culture (Fig. 6B). In confirmation of the

observed reductions in NFATc1 activity, expression of the NFATc1 regulated V-ATPase subunit d2 was also suppressed by Eriodictyol (Fig. 6B).

RANKL binding to cognate receptor RANK also results in activation of the transcription factor AP-1, via induction of the protein expression of critical component c-Fos. Western blot analysis of c-Fos protein expression showed that c-Fos was maximally induced on days 3 and 5 following RANKL stimulation of BMM (Fig. 6B). Treatment with Eriodictyol strongly blocked the expression of c-Fos relative to the RANKL-treated group. Collectively, these data demonstrate that Eriodictyol blocks the activation of NFATc1 and its downstream target V-ATPase-d2 via regulation of RANKL-induced NF- $\kappa$ B, MAPK, and  $Ca^{2+}$  pathways.

#### Eriodictyol inhibits RANKL-induced gene expression

Activation of NF- $\kappa$ B and NFATc1 results in the up-regulation of osteoclast marker gene expression. Based on the inhibitory effect of Eriodictyol on those pathways we investigated the effect of Eriodictyol (5 and 10  $\mu$ M) on osteoclastic gene expression. As shown in Figure 7, the expression of osteoclast marker genes (Ctsk, TRAcP, and V-ATPase-d2) was reduced dose dependently following treatment with Eriodictyol, suggesting that Eriodictyol attenuates osteoclast-specific gene expression.

#### Discussion

In adult skeleton bone remodeling is constantly active through coordinated balance between osteoclast-induced bone resorption and osteoblast-induced bone formation. When the balance is perturbed bone diseases such as osteoporosis are developed; these osteolytic diseases are associated with excessive osteoclastic activity (Boyle et al., 2003).

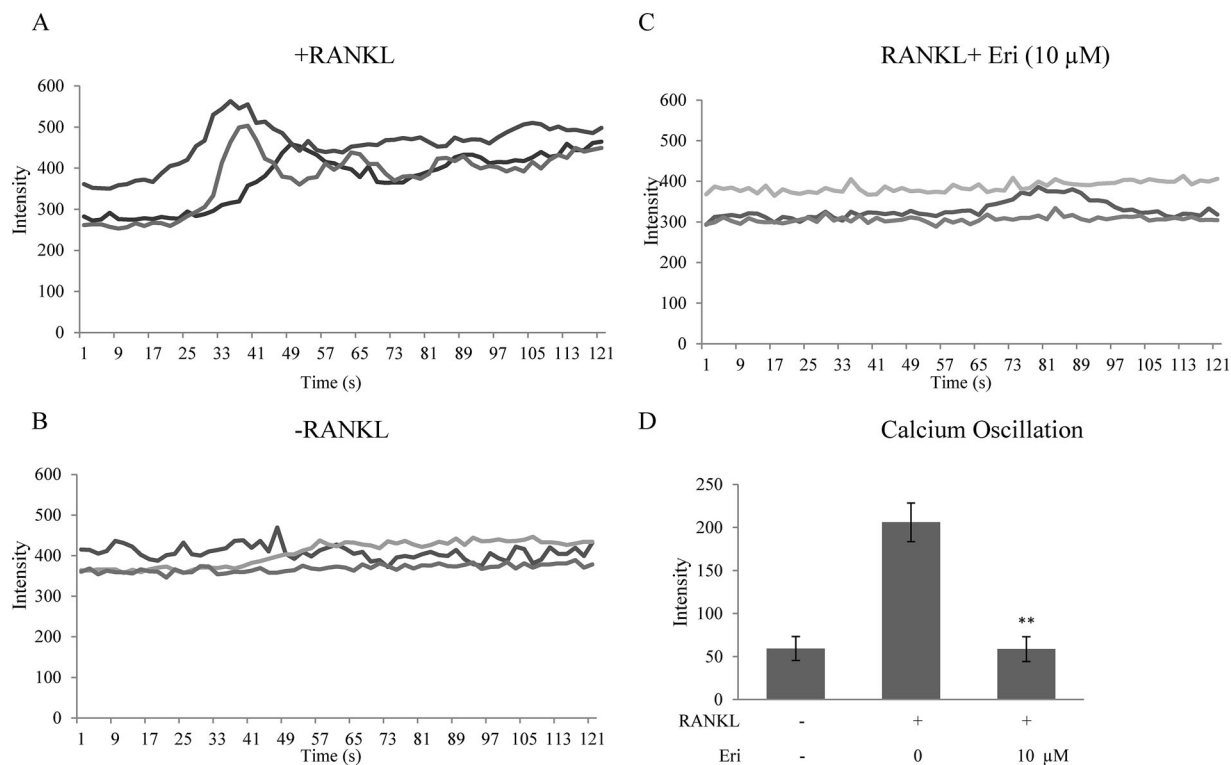


**Fig. 5.** Eriodictyol blocks RANKL-induced  $\text{Ca}^{2+}$  oscillation. BMMs were stimulated with GST-rRANKL (50 ng/mL) for 24 h and then calcium flux was assessed using Fluo4 calcium indicator. **A:** Representative calcium fluctuations within three cells treated with RANKL only. **B:** Representative calcium fluctuations within three cells treated with M-CSF only (negative control). **C:** Representative calcium fluctuations within three cells treated with RANKL and Eriodictyol (10  $\mu\text{M}$ ). **D:** Average change in intensity per cell. Calcium fluctuations were analysed across multiple cells for each condition and maximum peak intensity minus baseline intensity was calculated ( $n > 16$  individual cells/well, three wells/treatment) ( $n = 3$ ). “-” means RANKL untreated; “+” means RANKL treated. \*\* $P < 0.01$  relative to RANKL-stimulated controls.

Osteoclasts are formed by differentiation and fusion of macrophage precursor cells (Shinohara and Takayanagi, 2007). There are several cytokines that are critical for osteoclast differentiation, such as M-CSF, interleukin-1, transforming growth factor- $\beta$ , and RANKL. Of these factors, RANKL, in concert with its receptor RANK, has been identified as a key factor regulating both osteoclast formation in the presence of M-CSF, and inducing osteoclast activity (Lacey et al., 1998; Kong et al., 1999). As a critical regulator of both osteoclast formation and function, RANKL is an attractive target for treatment of osteolytic diseases.

Current therapies focus on inhibiting the resorptive function of osteoclasts. Several treatments are clinically available targeting bone disorders, including estrogen replacement therapy, bisphosphonates, and raloxifene. However, these treatments have some concerning side effects, including increased risk of breast cancer, gastrointestinal distress, and thromboembolism (Rodan and Martin, 2000; Rachner et al., 2011; Lippuner, 2012). Considering these concerns, it is important to search for alternative approaches for the treatment of excessive osteoclastic activity. Interestingly, due to the triggers of inflammation, cancer, and oxidative stress in the risk of bone loss, remarkable progress has been made in developing potent osteoclast inhibitor to inhibit those triggers (Abu-Amer, 2009; Wauquier et al., 2009). Of note, natural products exhibit a promising alternative treatment for bone diseases (Putnam et al., 2007). Recently, natural compounds like mangiferin, phloretin, and naringin, extracted from natural

plants, have been demonstrated to possess inhibitory effects on osteoclastic activity and may serve as potential therapies to treat skeletal diseases (Ang et al., 2011a,b; Kim et al., 2012). Therefore, we selected 20 compounds from commercial libraries for further study, based on their anti-inflammatory, anti-tumor or anti-oxidant benefits. For instance, germacrone inhibits human hepatoma cells growth via regulation of G2/M cell cycle and apoptosis (Liu et al., 2013); alpinetin exerts suppression effects on production of NO and PGE 2 in lipopolysaccharides induced RAW 264.7 cells (Lee et al., 2012); matrine prevents oxidative damage associated with the translocation of Nrf2 (Zhang et al., 2013). Through screening the effect of natural compounds on osteoclast formation, we observed that Eriodictyol significantly suppressed RANKL-induced osteoclastogenesis in a dose-dependent manner, with further work detailed in this manuscript showing the key mechanisms by which Eriodictyol exerts this action.

Mature osteoclasts express a variety of specialized proteins that play essential roles in the degradation of bone matrix, in particular, osteoclasts deficient in V-ATPase-d2 or Ctsk, exhibit dysfunctional bone resorption resulting in osteopetrosis (Gowen et al., 1999; Li et al., 1999). In the present study, we found that Eriodictyol abrogated the resorption of a hydroxyapatite substrate by mature osteoclasts as well as the expression of V-ATPase-d2 and Ctsk genes.

Dissecting the mechanism of action of an osteoclast inhibitor such Eriodictyol offers valuable information about the molecular targets of its actions. Eriodictyol suppresses many of

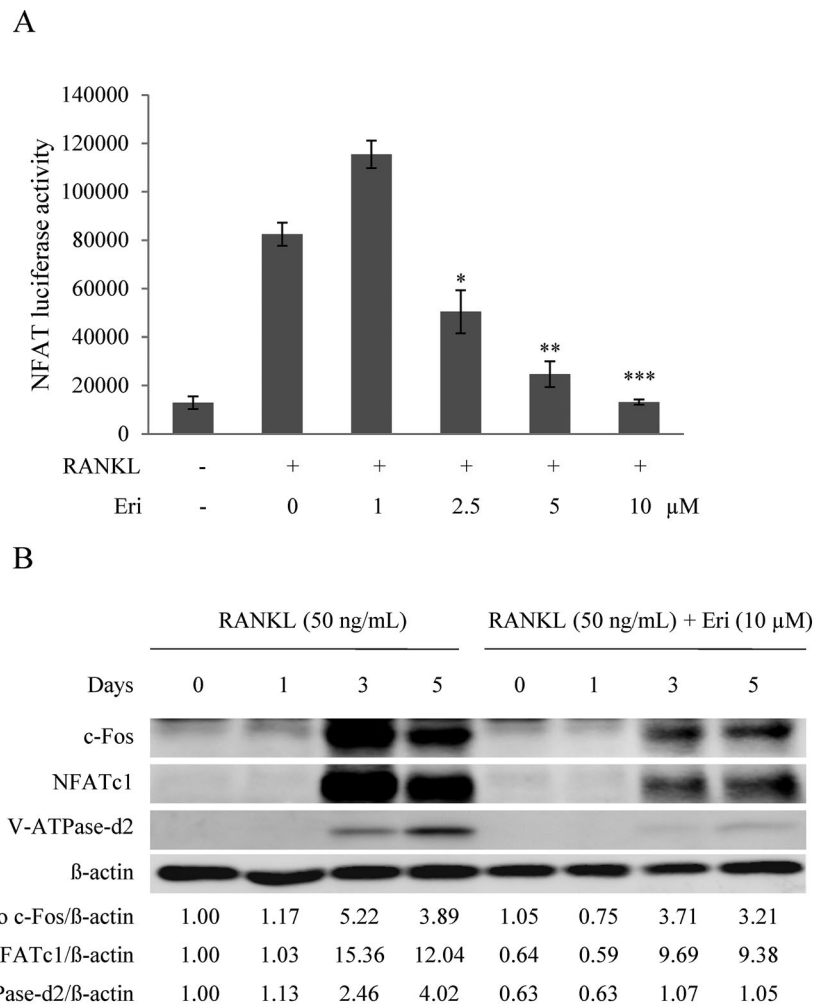


**Fig. 6. Eriodictyol abrogates RANKL-induced c-Fos and NFATc1 protein expression.** **A:** Luciferase activity in RANKL stimulated RAW264.7 cells transfected with an NFAT luciferase construct. Transfected cells were pre-treated with indicated concentrations of Eriodictyol, and subsequently stimulated with GST-rRANKL (50 ng/mL) ( $n = 3$ ). “-” means RANKL untreated; “+” means RANKL treated. \* $P < 0.05$ , \*\* $P < 0.01$ , \*\*\* $P < 0.001$  relative to RANKL-stimulated controls. **B:** Cell lysates from BMMs pre-treated with Eriodictyol (10 μM) and then stimulated with GST-rRANKL (50 ng/mL) for the indicated times. Western-blot was probed with c-Fos, NFATc1, V-ATPase-d2, and β-actin specific antibodies. Protein levels are expressed as the ratio relative to β-actin.

the critical pathways in osteoclast precursors, which explains its potency, but it is not clear at this stage what its main molecular target is in osteoclast precursors. RANK engagement by RANKL leads to recruitment of TRAF6, resulting in subsequent activation of IKK, which phosphorylates and degrades IκB-α to release the activated form of NF-κB. This is followed by translocation of NF-κB to the nucleus and subsequent activation of osteoclastogenesis gene transcription either directly or by inducing production of other transcription factors required for osteoclast formation and function (DiDonato et al., 1997). Deletion of p50 and p52 subunits of NF-κB in mice results in osteopetrosis, demonstrating that NF-κB acts as a significant regulator in the generation of osteoclasts (Boyce et al., 1999) and osteolytic bone conditions (Xu et al., 2009). In this study, Eriodictyol suppressed the activity of NF-κB, although Eriodictyol failed to prevent the degradation of IκB-α, perhaps indicating effects on NF-κB downstream of IκB. Since, several other pathways investigated here, including AP-1 and NFATc1 depend upon NF-κB activity, this may indicate that blockade of NF-κB is a

primary action of Eriodictyol. This compound has previously been found to suppress inflammatory responses (e.g., lipopolysaccharide-elicited responses) that depend on NF-κB (Lee, 2011). It is important to note; however, that RANKL signaling also activates supporting signaling pathways that are also required for successful osteoclast formation, notably MAPK and Ca<sup>2+</sup>-dependent pathways, which are not NF-κB dependent. This might indicate multiple molecular targets of Eriodictyol or effects upstream of NF-κB and MAPKs, perhaps involving TRAF6 or RANK.

The MAPK pathways play a crucial role in the modulation of osteoclast differentiation. Three MAPK pathways are relevant to osteoclast formation, namely ERK1/2, JNK, and p38, which are all activated by the binding of RANKL to RANK (Kobayashi et al., 2001). Inhibition of ERK activity affects both osteoclast survival and formation (Hotokezaka et al., 2002; Nakamura et al., 2003). Dominant-negative JNK abrogates RANKL-stimulated osteoclastogenesis, while activation of p38 exerts many effects on osteoclast differentiation but not on osteoclast function (Matsumoto et al., 2000; Li et al., 2002; Ikeda et al., 2004). In our

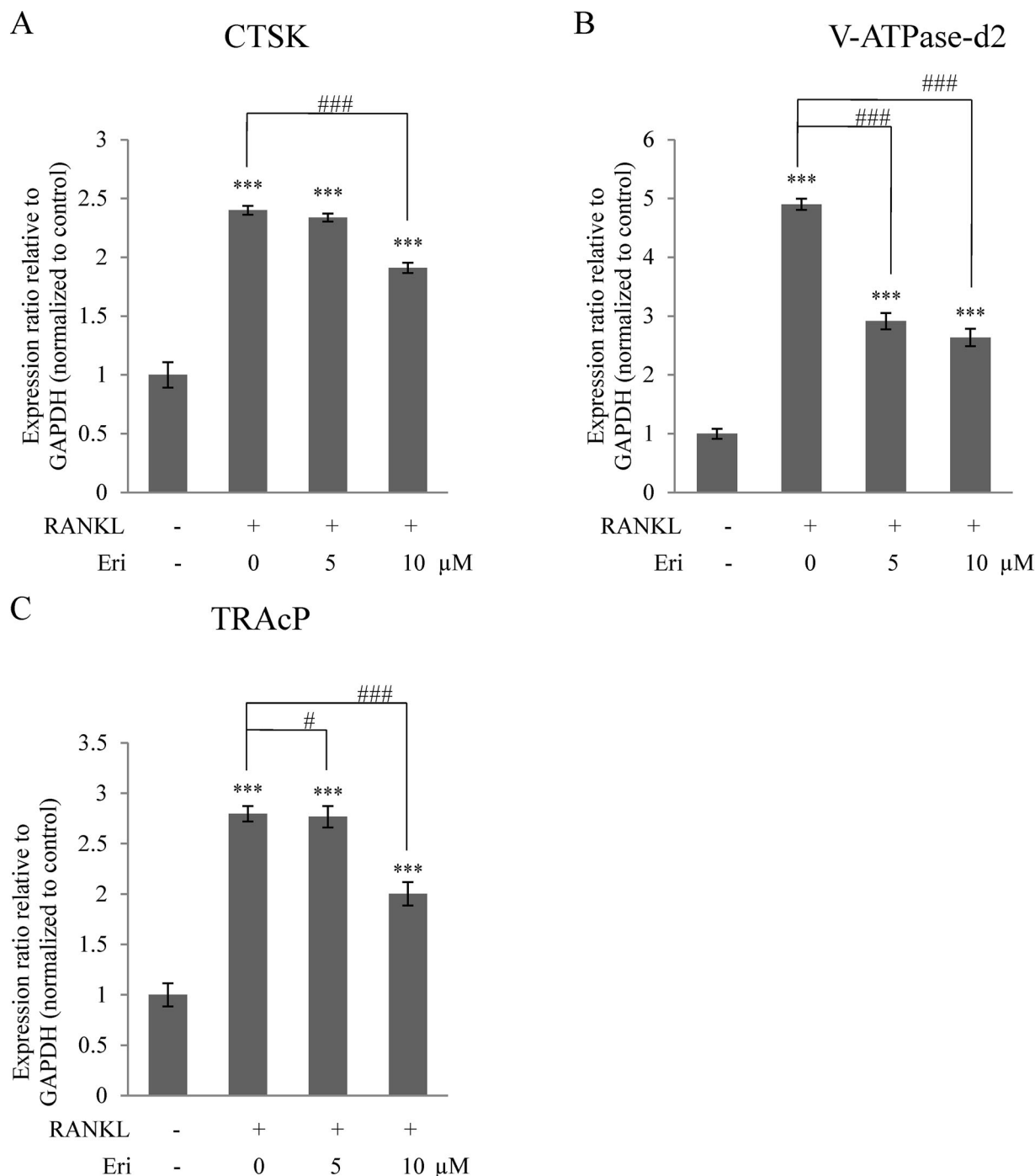


**Fig. 7. Eriodictyol reduces RANKL-induced gene expression in BMMs.** Relative levels of RANKL-induced gene expression in BMM cells treated with complete medium containing M-CSF and GST-rRANKL (50 ng/mL) in the presence or absence of indicated concentrations of Eriodictyol. Gene expression was normalized to GAPDH; (A) Ctsk (B) V-ATPase-d2, (C) TRAcP ( $n = 3$ ). “-” means RANKL untreated; “+” means RANKL treated. \* $P < 0.05$ , \*\* $P < 0.01$ , \*\*\* $P < 0.001$  relative to RANKL unstimulated controls. # $P < 0.05$ , ### $P < 0.01$ , #### $P < 0.001$  relative to RANKL-stimulated controls.

study, Eriodictyol inhibited RANKL-induced phosphorylation of ERK, JNK, and p38, implying that all of these pathways are affected and suggesting several ways that osteoclast formation is reduced by Eriodictyol.

RANKL treatment of BMMs also activates c-Fos, a component of the AP-1 transcription factor complex involved

in osteoclast and macrophage differentiation. Mice with mutations in c-Fos exhibit severe osteopetrotic diseases, due to reduced numbers of mature osteoclasts (Grigoriadis et al., 1994). In this study, we found that Eriodictyol strongly reduced the protein level of c-Fos, consistent with its inhibition of MAPK, and NF- $\kappa$ B pathways.

Along with inhibition of NF- $\kappa$ B, MAPKs, and c-Fos by Eriodictyol, we further examined its impact on NFATc1, a transcription factor that is indispensable for osteoclast formation. NFATc1 is a member of the NFAT family of proteins (NFATc1, NFATc2, NFATc3, NFATc4, and NFATc5). Importantly, NFATc1 is a master regulator of osteoclastogenesis, and can be spatio-temporally induced and activated by RANKL-stimulated signaling pathways (Shinohara and Takayanagi, 2007; Nakashima et al., 2012). NFATc1 can auto-regulate itself through binding motifs in promoter regions of its own gene and that of other NFAT family members (which bind a similar motif). It is notable that the NFATc1 promoter region can also recruit other transcription factors (NF- $\kappa$ B, NFATc2, and c-Fos) to amplify NFATc1 expression and downstream transcriptional processes (Asagiri et al., 2005; Aliprantis et al., 2008). Interestingly, ERK/MAPK, JNK/MAPK, and p38/MAPK also trigger induction of c-Fos and NFATc1 (Takayanagi et al., 2002; Ikeda et al., 2004; Monje et al., 2005; Huang et al., 2006). After activation of NFATc1, downstream osteoclastic genes are elicited, such as Ctsk, V-ATPase d2, and TRAcP (Balkan et al., 2009; Feng et al., 2009). Our study demonstrated that Eriodictyol inhibited the protein level of NFATc1 with associated down-regulation of osteoclast-specific genes. From the combined suppression of osteoclastic genes (Ctsk, V-ATPase-d2, and TRAcP) and suppression of NF- $\kappa$ B activity, MAPKs, and c-Fos level by Eriodictyol, it was inferred that Eriodictyol attenuated the process of RANKL signaling (NF- $\kappa$ B and MAPK pathway), followed by suppression of the induction of c-Fos, finally, down-regulation of NFATc1. In addition to the above observations with NF- $\kappa$ B and MAPK, NFATc1 is also sensitive to the release of intracellular  $Ca^{2+}$  during osteoclast differentiation. RANKL-induced  $Ca^{2+}$  oscillation activates the auto-amplification loop of NFATc1 required for osteoclastogenesis (Takayanagi et al., 2002; Negishi-Koga and Takayanagi, 2009). We found that Eriodictyol could inhibit the intensity of  $Ca^{2+}$  oscillation in response to RANKL, congruent with the pivotal role of Calcium signaling-induced stimulation of NFATc1 (Takayanagi et al., 2002; Koga et al., 2004).

In summary, we observed that Eriodictyol prevented RANKL-induced osteoclast formation and function through inhibiting NFATc1 activity and RANKL-induced NF- $\kappa$ B, MAPK, and  $Ca^{2+}$  signaling. Our study highlighted that the regulation of the transcription factor NFATc1 is a master switch in the course of RANKL-induced osteoclastogenesis. Our findings thus provide a cellular and molecular mechanism for the inhibitory effect of Eriodictyol on RANKL-induced osteoclastogenesis. Future studies are required to elucidate the effect of Eriodictyol on osteoblast function and the metabolism of Eriodictyol in vitro/vivo to confirm its suitability as a potential treatment against osteolytic bone diseases. Thus, Eriodictyol could offer a promising therapeutic strategy against osteoporosis and other osteoclast-related diseases.

## Acknowledgments

This study was funded by the National Health and Medical Research Council of Australia, Natural Science Foundation of Guangxi Province (No. 2015GXNSFDA139019) and Innovation Project of Guangxi Graduate Education. This study is also sponsored in part by Co-innovation Centre for Bio-Medicine, Guangxi Key Laboratory of Regenerative Medicine, Guangxi Medical University. Fangming Song and Jiaka Xu made mutual collaborative visits in 2015.

## Literature Cited

Abu-Amer Y. 2009. Inflammation, cancer, and bone loss. *Curr Opin Pharmacol* 9:427–433.  
 Aliprantis AO, Ueki Y, Sulyanto R, Park A, Sigris KS, Sharma SM, Ostrowski MC, Olsen BR, Glimcher LH. 2008. NFATc1 in mice represses osteoprotegerin during

osteoclastogenesis and dissociates systemic osteopenia from inflammation in cherubism. *J Clin Invest* 118:3775–3789.  
 Ang ES, Liu Q, Qi M, Liu HG, Yang XH, Chen HH, Zheng MH, Xu J. 2011a. Mangiferin attenuates osteoclastogenesis, bone resorption, and RANKL-induced activation of NF- $\kappa$ B and ERK. *J Cell Biochem* 112:89–97.  
 Ang ES, Yang X, Chen H, Liu Q, Zheng MH, Xu J. 2011b. Naringin abrogates osteoclastogenesis and bone resorption via the inhibition of RANKL-induced NF- $\kappa$ B and ERK activation. *FEBS Lett* 585:2755–2762.  
 Asagiri M, Sato K, Usami T, Ochi S, Nishina H, Yoshida H, Morita I, Wagner EF, Mak TW, Serfling E, Takayanagi H. 2005. Autoamplification of NFATc1 expression determines its essential role in bone homeostasis. *J Exp Med* 202:1261–1269.  
 Balkan W, Martinez AF, Fernandez I, Rodriguez MA, Pang M, Troen BR. 2009. Identification of NFAT binding sites that mediate stimulation of cathepsin K promoter activity by RANK ligand. *Gene* 446:90–98.  
 Baud'huin M, Duplomb L, Ruiz Velasco C, Fortun Y, Heymann D, Padrines M. 2007. Key roles of the OPG-RANK-RANKL system in bone oncology. *Expert Rev Anticancer Ther* 7:221–232.  
 Boyce BF, Xing L, Franzoso G, Siebenlist U. 1999. Required and nonessential functions of nuclear factor- $\kappa$ B in bone cells. *Bone* 25:137–139.  
 Boyle WJ, Simonet WS, Lacey DL. 2003. Osteoclast differentiation and activation. *Nature* 423:337–342.  
 DiDonato JA, Hayakawa M, Rothwarf DM, Zandi E, Karin M. 1997. A cytokine-responsive I $\kappa$ B kinase that activates the transcription factor NF- $\kappa$ B. *Nature* 388:548–554.  
 Feng H, Cheng T, Steer JH, Joyce DA, Pavlos NJ, Leong C, Kular J, Liu J, Feng X, Zheng MH, Xu J. 2009. Myocyte enhancer factor 2 and microphthalmia-associated transcription factor cooperate with NFATc1 to transactivate the V-ATPase d2 promoter during RANKL-induced osteoclastogenesis. *J Biol Chem* 284:14667–14676.  
 Gowen M, Lazner F, Dodds R, Kapadia R, Feild J, Tavaria M, Bertonecello I, Drake F, Zavorsell S, Tellis I, Hertzog P, Debouck C, Kola I. 1999. Cathepsin K knockout mice develop osteopetrosis due to a deficit in matrix degradation but not demineralization. *J Bone Miner Res* 14:1654–1663.  
 Grigoriadis AE, Wang ZQ, Cecchini MG, Hofstetter W, Felix R, Fleisch HA, Wagner EF. 1994. C-Fos: A key regulator of osteoclast-macrophage lineage determination and bone remodeling. *Science* 266:443–448.  
 Hotokezaka H, Sakai E, Kanaoka K, Saito K, Matsuo K, Kitaura H, Yoshida N, Nakayama K. 2002. U0126 and PD98059, specific inhibitors of MEK, accelerate differentiation of RAW264.7 cells into osteoclast-like cells. *J Biol Chem* 277:47366–47372.  
 Huang H, Ryu J, Ha J, Chang EJ, Kim HJ, Kim HM, Kitamura T, Lee ZH, Kim HH. 2006. Osteoclast differentiation requires TAK1 and MKK6 for NFATc1 induction and NF- $\kappa$ B transactivation by RANKL. *Cell Death Differ* 13:1879–1891.  
 Ikeda F, Nishimura R, Matsubara T, Tanaka S, Inoue J, Reddy SV, Hata K, Yamashita K, Hiraga T, Watanabe T, Kukita T, Yoshioka K, Rao A, Yoneda T. 2004. Critical roles of c-Jun signaling in regulation of NFAT family and RANKL-regulated osteoclast differentiation. *J Clin Invest* 114:475–484.  
 Kim JL, Kang MK, Gong JH, Park SH, Han SY, Kang YH. 2012. Novel antiosteoclastogenic activity of phloretin antagonizing RANKL-induced osteoclast differentiation of murine macrophages. *Mol Nutr Food Res* 56:1223–1233.  
 Kobayashi N, Kadono Y, Naito A, Matsumoto K, Yamamoto T, Tanaka S, Inoue J. 2001. Segregation of TRAF6-mediated signaling pathways clarifies its role in osteoclastogenesis. *EMBO J* 20:1271–1280.  
 Koga T, Inui M, Inoue K, Kim S, Suematsu A, Kobayashi E, Iwata T, Ohnishi H, Matozaki T, Kodama T, Taniguchi T, Takayanagi H, Takai T. 2004. Costimulatory signals mediated by the ITAM motif cooperate with RANKL for bone homeostasis. *Nature* 428:758–763.  
 Kong YY, Yoshida H, Sarosi I, Tan HI, Timms E, Capparelli C, Morony S, Oliveira-dos-Santos AJ, Van G, Itie A, Khoo W, Wakeham A, Dunstan CR, Lacey DL, Mak TW, Boyle WJ, Penninger JM. 1999. OPG is a key regulator of osteoclastogenesis, lymphocyte development and lymph-node organogenesis. *Nature* 397:315–323.  
 Kular J, Tickner J, Chim SM, Xu J. 2012. An overview of the regulation of bone remodelling at the cellular level. *Clin Biochem* 45:863–873.  
 Lacey DL, Timms E, Tan HL, Kelley MJ, Dunstan CR, Burgess T, Elliott R, Colombero A, Elliott G, Scully S, Hsu H, Sullivan J, Hawkins N, Davy E, Capparelli C, Eli A, Qian YX, Kaufman S, Sarosi I, Shalhoub V, Senaldi G, Guo J, Delaney J, Boyle WJ. 1998. Osteoprotegerin ligand is a cytokine that regulates osteoclast differentiation and activation. *Cell* 93:165–176.  
 Lee E, Jeong KW, Shin A, Jin B, Inawali HN, Jun BH, Lee JY, Heo YS, Kim Y. 2013. Binding model for eriodictyol to Jun-N terminal kinase and its anti-inflammatory signaling pathway. *BMB Rep* 46:594–599.  
 Lee JK. 2011. Anti-inflammatory effects of eriodictyol in lipopolysaccharide-stimulated raw 264.7 murine macrophages. *Arch Pharm Res* 34:671–679.  
 Lee MY, Seo CS, Lee JA, Shin IS, Kim SJ, Ha H, Shin HK. 2012. Alpina katsumadai H (AYATA) seed extract inhibit LPS-induced inflammation by induction of heme oxygenase-1 in RAW264.7 cells. *Inflammation* 35:746–757.  
 Lee SE, Yang H, Son GW, Park HR, Park CSYH, Park YS. 2015. Eriodictyol protects endothelial cells against oxidative stress-induced cell death through modulating ERK/NRF2/ARE-dependent heme oxygenase-1 expression. *Int J Mol Sci* 16:14526–14539.  
 Li X, Udagawa N, Itoh K, Suda K, Murase Y, Nishihara T, Suda T, Takahashi N. 2002. P38 MAPK-mediated signals are required for inducing osteoclast differentiation but not for osteoclast function. *Endocrinology* 143:3105–3113.  
 Li YP, Chen W, Liang Y, Li E, Stashenko P. 1999. Atp6i-deficient mice exhibit severe osteopetrosis due to loss of osteoclast-mediated extracellular acidification. *Nat Genet* 23:447–451.  
 Lippuner K. 2012. The future of osteoporosis treatment—A research update. *Swiss Med Wkly* 142:w13624.  
 Liu Y, Wang W, Fang B, Ma F, Zheng Q, Deng P, Zhao S, Chen M, Yang G, He G. 2013. Anti-tumor effect of garmacron on human hepatoma cell lines through inducing G2/M cell cycle arrest and promoting apoptosis. *Eur J Pharmacol* 698:95–102.  
 Manolagas SC, Jilka RL. 1995. Bone marrow, cytokines, and bone remodeling. Emerging insights into the pathophysiology of osteoporosis. *N Engl J Med* 332:305–311.  
 Matsumoto M, Sudo T, Saito T, Osada H, Tsujimoto M. 2000. Involvement of p38 mitogen-activated protein kinase signaling pathway in osteoclastogenesis mediated by receptor activator of NF- $\kappa$ B ligand (RANKL). *J Biol Chem* 275:31155–31161.  
 Monje P, Hernandez-Losa J, Lyons RJ, Castellone MD, Gutkind JS. 2005. Regulation of the transcriptional activity of c-Fos by ERK. A novel role for the prolyl isomerase PIN1. *J Biol Chem* 280:35081–35081.  
 Nakamura H, Hirata A, Tsuji T, Yamamoto T. 2003. Role of osteoclast extracellular signal-regulated kinase (ERK) in cell survival and maintenance of cell polarity. *J Bone Miner Res* 18:1198–1205.  
 Nakashima T, Hayashi M, Takayanagi H. 2012. New insights into osteoclastogenic signaling mechanisms. *Trends Endocrinol Metab* 23:582–590.

- Negishi-Koga T, Takayanagi H. 2009.  $\text{Ca}^{2+}$ -NFATc1 signaling is an essential axis of osteoclast differentiation. *Immunol Rev* 231:241–256.
- Putnam SE, Scutt AM, Bicknell K, Priestley CM, Williamson EM. 2007. Natural products as alternative treatments for metabolic bone disorders and for maintenance of bone health. *Phytother Res* 21:99–112.
- Rachner TD, Khosla S, Hofbauer LC. 2011. Osteoporosis: Now and the future. *Lancet* 377:1276–1287.
- Rodan GA, Martin TJ. 2000. Therapeutic approaches to bone diseases. *Science* 289:1508–1514.
- Shinohara M, Takayanagi H. 2007. Novel osteoclast signaling mechanisms. *Curr Osteoporos Rep* 5:67–72.
- Takayanagi H. 2007. Osteoimmunology: Shared mechanisms and crosstalk between the immune and bone systems. *Nat Rev Immunol* 7:292–304.
- Takayanagi H, Kim S, Koga T, Nishina H, Isshiki M, Yoshida H, Saiura A, Isobe M, Yokochi T, Inoue J, Wagner EF, Mak TW, Kodama T, Taniguchi T. 2002. Induction and activation of the transcription factor NFATc1 (NFAT2) integrate RANKL signaling in terminal differentiation of osteoclasts. *Dev Cell* 3:889–901.
- Teitelbaum SL. 2000. Bone resorption by osteoclasts. *Science* 289:1504–1508.
- van der Kraan AG, Chai RC, Singh PP, Lang BJ, Xu J, Gillespie MT, Price JT, Quinn JM. 2013. HSP90 inhibitors enhance differentiation and MITF (microphthalmia transcription factor) activity in osteoclast progenitors. *Biochem J* 451:235–244.
- Wang C, Steer JH, Joyce DA, Yip KH, Zheng MH, Xu J. 2003. 12-O-tetradecanoylphorbol-13-acetate (TPA) inhibits osteoclastogenesis by suppressing RANKL-induced NF-kappaB activation. *J Bone Miner Res* 18:2159–2168.
- Wauquier F, Leotoing L, Coxam V, Guicheux J, Wittrant Y. 2009. Oxidative stress in bone remodelling and disease. *Trends Mol Med* 15:468–477.
- Xu J, Tan JW, Huang L, Laird XH G, Liu R, Wysocki D, Zheng S. 2000. Cloning, sequencing, and functional characterization of the rat homologue of receptor activator of NF-kappaB ligand. *J Bone Miner Res* 15:2178–2186.
- Xu J, Wu HF, Ang ES, Yip K, Woloszyn M, Zheng MH, Tan RX. 2009. NF-kappaB modulators in osteolytic bone diseases. *Cytokine Growth Factor Rev* 20:7–17.
- Zhang HF, Shi LJ, Song GY, Cai ZG, Wang C, An RJ. 2013. Protective effects of matrine against progression of high-fructose diet-induced steatohepatitis by enhancing antioxidant and anti-inflammatory defences involving Nrf2 translocation. *Food Chem Toxicol* 55:70–77.

### Supporting Information

Additional supporting information may be found in the online version of this article at the publisher's web-site.